

Generalized Analysis and Optimization of D2D Communications in Cellular Networks

Imène Trigui, Member, *IEEE*, and Sofiène Affes, Senior Member, *IEEE*,

Abstract—This paper develops an innovative approach to the modeling and analysis of downlink cellular networks with device-to-device (D2D) transmissions. The analytical embodiment of the signal-to-noise and-interference ratio (SINR) analysis in general fading channels is unified due to the H-transform theory, a taxonomy never considered before in stochastic geometry-based cellular network modeling and analysis. Whereas ubiquitous results for coverage probability have a double integral, ones derived here for D2D and cellular coverage have compact or even closed forms, while subsuming those previously presented for all the known simple and composite fading models. By harnessing its tractability, the developed statistical machinery is employed to launch an investigation into the optimal design of coexisting D2D and cellular communications. We propose novel coverage-aware power control combined with opportunistic access control to maximize the area spectral efficiency (ASE) of D2D communications. Simulation results substantiate performance gains achieved by the proposed optimization framework in terms of cellular communication coverage probability, average D2D transmit power, and the ASE of D2D communications under different fading models and link- and network-level dynamics.

I. INTRODUCTION

The recent sky-rocketing data demand has compelled both industry and regulatory bodies to come up with new paradigm-shifting technologies able to keep pace with such stringent requirements and cope with the massive connectivity characterizing future 5G networks. Currently being touted as a strong contender for 5G networks [1], [2], device-to-device (D2D) communications allow direct communication between cellular mobiles, thus bypassing the network infrastructure, resulting in shorter transmission distances and improved data rates than traditional cellular networks.

In the past few years, D2D-enabled networks have been actively studied by the research community. For example, in [3], it was shown that by allowing radio signals to be relayed by mobiles, D2D communications can improve spectral efficiency and the coverage of conventional cellular networks. Additionally, D2D has been applied to machine-to-machine (M2M) communications [4] and proposed as a possible enabler of vehicle-to-vehicle (V2V) applications [5]. More recent works [6]- [8] have modeled the user locations with PPP distributions and analytically tackled D2D communication by harnessing the powerful stochastic geometry tools.

Notwithstanding these advances, computing the SINR in randomly deployed networks, namely D2D-enabled cellular networks, has been successfully tractable only for fading

channels and transmission schemes whose equivalent per-link power gains follow a Gamma distribution with integer shape parameter ([9] and references therein), while much work has been achieved on evaluating the performance of D2D networks over Rayleigh fading channels [6]. Such particular fading distributions have very often limited legitimacy according to [10], [11], who argued that these fading models may fail to capture new and more realistic fading environments. This is particularly true as new communication technologies accommodating a wide range of usage scenarios with diverse link requirements are continuously being introduced and analyzed, for example, body-centric and millimeter-wave communications. Recently few works have been conducted to consider D2D networks with general fading channels [12]- [15]. However, besides being channel-model-dependent, these works relied on series representation methods (e.g., infinite series in [14] and Laguerre polynomial series in [13], [15]) thereby expressing the interference functionals as an infinite series of higher order derivative terms given by the Laplace transform of the interference power. These methods cannot lend themselves to closed-form expressions and, hence, require complex numerical evaluation.

For the successful coexistence of D2D and cellular users, efficient interference management, e.g., through power or access control, is required. Recently, extensive research on power allocation strategies aiming to maximize the spectral efficiency of D2D communication in random network models were studied and analyzed [16]- [18]. In [16], channel-aware power control algorithms aiming to maximize the D2D sum rate are proposed and analyzed using stochastic geometry. In [17], SIR-aware access scheme based on the conditional coverage probability of D2D underlaid cellular networks is proposed to increase the aggregate rate of D2D links. Similarly, [18] proposes to enhance the sum rate of D2D links by optimally finding groups and access probabilities. To the best of the authors' knowledge, none of these works consider generalized fading channels when proposing access and power control schemes to accommodate multiple D2D pairs underlaid in a cellular network. Yet, these works only focused on the simplistic Rayleigh fading.

In this paper, we focus on the design of access control and power allocation strategies for D2D communication underlaying wireless networks under generalized fading conditions, an uncharted territory wherein the throughput potential of such networks remains unquantified. The contributions of this paper are as follows:

- We propose an analytical framework based on newly established tools from stochastic geometry analysis [9]

Work supported by the Discovery Grants and the CREATE PERSWADE (www.create-perswade.ca) programs of NSERC, and a Discovery Accelerator Supplement (DAS) Award from NSERC.

to evaluate the cellular and D2D SINR distributions in general fading conditions embodying the H-transform theory. We establish extremely useful results for the SINR and interference distributions never reported previously in the literature.

- We successfully unify our analysis framework in the sense that it can be applied for any fading channel whose envelope follows the form of $x^\beta e^{-\lambda x} H(cx^\zeta)$, where $H(\cdot)$ stands for the Fox-H function [19], e.g., Nakagami- m , Weibull, or κ - μ and shadowed κ - μ to account for various small-scale fading effects such as LOS/NLOS (line-of-sight/non-LOS) conditions, multipath clustering, composite fading in specular or inhomogeneous radio propagation, and power imbalance between the in-phase and quadrature signal components.
- In order to guarantee the coverage probability of cellular users in a distributed manner, we derive the interference budget of a typical D2D link, which represents the allowable transmit power level of D2D transmitters. We formulate an optimization problem to find the access probability which maximizes the average area spectral efficiency utility of D2D communication underlying multiple cells subject to cellular coverage-aware power budget. The proposed opportunistic access requires only statistical CSI (channel state information), in contrast to the centralized resource allocation which requires full CSI, thereby inducing less delay in the network.
- We derive simple expressions for the optimal access probability and D2D coverage-aware power budget based on an approximation of the D2D coverage probability under both Nakagami- m and Weibull fading channels. The developed machinery is prone to handle more comprehensive fading models, namely the shadowed κ - μ .

The remainder of this paper is organized as follows. We describe the system model in Section II. In Section III, we put forward the fading model-free statistical distribution of cellular and D2D links in Section III, then we put forth the unifying H-transform analysis over the considered fading channels. We exploit in Section VI the developed statistical machinery to present the cellular coverage-aware power control and ASE of D2D communications under different fading conditions. We present numerical results in Section V and conclude the paper in Section VII with some closing remarks.

II. SYSTEM MODEL

We envision a D2D-enabled cellular network model in which the locations of macro BSs (MBS) and D2D users are distributed according to the independent homogeneous PPPs (HPPPs) Ψ_c and Ψ_d with intensities λ_c and λ_d , respectively, where $\lambda_d \gg \lambda_c$. Each user associates with the nearest MBS while allowed to connect to any D2D transmitter (Tx) without any restriction (open access strategy). We assume that both the cellular and D2D links experience channel impairments including path loss and small-scale fading. The received power from the MBS/D2D Tx located at $Z_x \in \Psi_x$, $x = \{c, d\}$ is given as $P(Z_x) = P_x h_x \|Z_x\|^{-\alpha}$, where P_c and P_d are the transmit powers of the MBS and D2D Txs, respectively,

$\alpha \geq 2$ is the pathloss exponent and h_x is an i.i.d. sequence of random variables modeling small scale fading and shadowing. We assume that there is universal frequency reuse across the network, but the number of resource blocks is greater than the number of users within the cell and hence, there is no intra-cell interference. The signal-to-interference plus noise ratio (SINR) experienced by a typical user at origin can be expressed as:

$$\text{SINR}_x = \frac{P_x h_x \|Z_x^*\|^{-\alpha}}{\sigma^2 + I_x}, \quad (1)$$

where, $r = \|Z_x^*\|$, $x = \{c, d\}$ is the distance to the nearest MBS ($Z_c^* = \arg \max_{Z_c \in \Psi_c} P_c \|Z_c\|^{-\alpha}$) and to the typical D2D Tx that delivers the maximum received SINR, respectively. The co-channel interference from other D2D pairs to the probe D2D receiver or from other MBS to the probe cellular receiver are denoted by $I_x = \sum_{Z_x \in \Psi_x \setminus Z_x^*} P_x h_x \|Z_x\|^{-\alpha}$.

III. GENERALIZED SINR ANALYSIS

Theorem 1: The SINR complementary cumulative distribution function (CCDF) of D2D and cellular links, defined as $\mathbb{P}^x(T) \triangleq \mathbb{P}\left(\text{SINR}_x = \frac{P_x^r}{I_x + \sigma^2} \geq T\right)$ for $x \in \{d, c\}$, is given by

$$\begin{aligned} \mathbb{P}^x(T) &= \frac{1}{T} \int_0^\infty \underbrace{\mathcal{E}_h \left[h \text{H}_{1,2}^{1,0} \left[\frac{h\xi}{T} \middle| \begin{matrix} (0, 1) \\ (0, 1), (-1, 1) \end{matrix} \right] \right]}_{\Psi(\xi, T)} \\ &\quad \times \mathcal{E}_r \left[\exp \left(-\frac{\sigma^2}{P_x} \xi r^\alpha - \mathcal{A}^x(\xi r^\alpha, \delta) \right) \right] d\xi, \quad (2) \end{aligned}$$

where $\delta = \frac{2}{\alpha}$, $\mathcal{E}_z[\cdot]$ is the expectation with respect to the random variable z , $\text{H}_{a,b}^{c,d}[\cdot]$ denotes the Fox-H function [20], [19] and

$$\begin{cases} \mathcal{A}^d(\xi, \delta) = \pi \lambda_d \xi^\delta \Gamma(1 - \delta) \mathcal{E}[h^\delta], & \text{D2D;} \\ \mathcal{A}^c(\xi, \delta) = \frac{\pi \delta \lambda_c \xi \mathcal{E}_h \left[h {}_2F_2 \left(1 - \delta, 1; 2 - \delta, 2; -\frac{\xi h}{r^{2/\delta}} \right) \right]}{r^{2(1/\delta - 1)}(1 - \delta)}, & \text{Cellular.} \end{cases} \quad (3)$$

whereby ${}_pF_q(\cdot)$ and $\Gamma(\cdot)$ stand for the generalized hypergeometric [21, Eq. (9.14.1)] and the incomplete gamma [21, Eq.(8.310.1)] functions, respectively.

Proof: See Appendix A for details.

Theorem 1 demonstrates the general expressions of the Laplace transforms of I_d and I_c as well as the D2D and cellular SINR CCDFs without assuming any specific random channel gain and distance models¹.

Notice that $\Psi(\xi, T)$ in (2) is an integral transform that involves the Fox's H-function as kernel, whence called H-transform. The H-transforms involving Fox's H-functions as kernels were first suggested by Verma [22] with the help of \mathcal{L}_2 -theory for integral transforms in the Lebesgue space \mathcal{L}_2 [22]. So far, integral transforms, such as the classical Laplace, Mellin, and Hankel transforms have been used successfully in solving many problems pertaining to stochastic geometry modeling in cellular networks (cf. [6] and [9] and references

¹In this paper, the unbounded pathloss model is used due to its mathematical tractability. However more realistic models notably bounded pathloss models (BPM) $((1+d)^{-\alpha}, \min(1, r^{-\alpha}))$ can be studied through the general SINR expression in Theorem 1.

therein). However, to the best of our knowledge, this paper is the first to introduce the Fox's-H function and H-transforms to cellular network analysis. Since H-functions subsume most of the known special functions including Meijer's G-functions [20], then by virtue of the essential so-called Mellin operation, involved in the Mellin transform of two H-functions, $\Psi(\xi, T)$ culminate in a H-function for any channel model with probability density function (PDF) $f_h(\cdot)$.

A single H-variate PDF considers homogeneous radio propagation conditions and captures composite effects of multipath fading and shadowing, subsuming most of typical models such as Rayleigh, Nakagami- m , Weibull, N -Nakagami- m , (generalized) \mathcal{K} -fading, and Weibull/gamma fading [23] as its special cases.

In contrast, to characterize specular and/or inhomogeneous environments, the multipath component consists of a strong LOS or specularly-reflected wave as well as unequal-power or correlated in-phase and quadrature scattered waves [10], [23], [24]. Another class of H-variate (degree-2) PDF that is the product of an exponential function and a Fox's H-function is used to account for specular or inhomogeneous radio propagation conditions including a variety of relevant models such as Rician, κ - μ , Rician/LOS gamma, and κ - μ /LOS gamma (or κ - μ shadowed) fading [10], [24] as special cases.

In this paper, we choose, however, to work with single H-variate fading PDFs to keep the presentation as compact as possible. Some other fading models that can still be considered within the framework of this paper are degree-2 H-variate fading models including the κ - μ and the shadowed κ - μ . We illustrate this fact in Appendix D.

Proposition 1 (Nakagami- m Fading): The D2D and cellular SINR CCDFs over Nakagami- m fading are given by

$$\mathbb{P}_m^x(T) = \frac{\pi\delta\lambda_x \left(\frac{\sigma^2}{P_x}\right)^{\delta/2}}{\Gamma(m)} \int_0^\infty \frac{H_{1,1}^{0,1} \left[\frac{\Omega\xi}{mT} \middle| \begin{matrix} (1-m, 1) \\ (0, 1) \end{matrix} \right]}{\xi^{1+\frac{\delta}{2}}} H_{1,1}^{1,1} \left[\pi\lambda_x (1 + \mathcal{Q}_x) \frac{\left(\frac{\sigma^2}{P_x}\right)^\delta}{\xi^\delta} \middle| \begin{matrix} (1-\delta, \delta) \\ (0, 1) \end{matrix} \right] d\xi, \quad (4)$$

where $x \in \{c, d\}$, and

$$\begin{cases} \mathcal{Q}_d = \xi^\delta \left(\frac{\Omega}{m}\right)^\delta \frac{\Gamma(1-\delta)\Gamma(m+\delta)}{\Gamma(m)}, \\ \mathcal{Q}_c = \frac{\delta\xi\Omega}{(1-\delta)} {}_3F_2(1-\delta, 1, m+1; 2-\delta, 2; -\frac{\Omega\xi}{m}). \end{cases} \quad (5)$$

Proof: See Appendix B for details.

Definition 1: Consider the Fox's-H function $H_{p,q}^{m,n} \left[x \middle| \begin{matrix} (a_1, A_1), \dots, (a_n, A_n) \\ (b_1, b_1), \dots, (b_n, b_n) \end{matrix} \right]$ defined by [25, Eq. (1.1.1)]. It's asymptotic expansion near $x = \infty$ is given by [25, Eq. (1.5.9)] as

$$H_{p,q}^{m,n}(x) \underset{x \rightarrow \infty}{\approx} \eta x^d, \quad (6)$$

where $d = \max \left(\frac{a_i-1}{A_i} \right)$, $i = 1, \dots, n$ and η is calculated as in [25, Eq. (1.5.10)].

Corollary 1 (Limits of Network Densification in Nakagami- m Fading): The downlink SINR saturates past a certain network density as

$$\lim_{\lambda_c \rightarrow \infty} \mathbb{P}_m^c(T) = \frac{\left(\frac{P_c}{\sigma^2}\right)^{\delta/2}}{\Gamma(m)} \int_0^\infty \frac{H_{1,1}^{0,1} \left[\frac{\Omega\xi}{mT} \middle| \begin{matrix} (1-m, 1) \\ (0, 1) \end{matrix} \right]}{\xi^{1-\frac{\delta}{2}} (1 + \mathcal{Q}_c)} dx. \quad (7)$$

Proof: Applying (6) to (46) when $\lambda_c \rightarrow \infty$ yields the result after recognizing that $d = -1$ and $\eta = \frac{1}{\delta}$.

Corollary 1 proves that at some point ultra-densification will no longer be able to deliver significant coverage gains. Although, some other works have also identified such fundamental scaling regime for network densification [6],[9], its network performance limits in terms of coverage have never been exactly quantified as in Corollary 1.

Due to potentially high density of devices, D2D networks are overwhelmingly interference-limited. In this respect, the D2D SIR distribution becomes

$$\mathbb{P}_m^{d, \sigma^2 \simeq 0}(T) \stackrel{(a)}{=} \frac{1}{\Gamma(m)} \mathcal{E}_{r_d} \left[H_{2,2}^{2,0} \left[\lambda_d \pi \kappa_m T^\delta r^2 \middle| \begin{matrix} (1, \delta) \\ (0, 1), (m, \delta) \end{matrix} \right] \right], \quad (8)$$

where (a) follows form (46) when $\sigma^2 \simeq 0$ by resorting to [20, Eq.(2.19)] with $\kappa_m = \frac{\Gamma(1-\delta)\Gamma(m+\delta)}{\Gamma(m)}$. The analytical result in (8) applies to any spatial distribution of r_d . It derives under Rayleigh distance, using [20, Eq.(2.19)], as

$$\mathbb{P}_m^{d, \sigma^2 \simeq 0}(T) = \frac{1}{\Gamma(m)} H_{2,2}^{2,1} \left[\kappa_m T^\delta \middle| \begin{matrix} (0, 1), (1, \delta) \\ (0, 1), (m, \delta) \end{matrix} \right]. \quad (9)$$

Proposition 2 (Weibull Fading): The Weibull fading channel accounts for the nonlinearity of a propagation medium with a physical fading parameters ν . When h follows a Weibull distribution with parameters $(\nu, \Phi = \Omega^\nu)$ [23], then the SINR CCDFs of D2D and cellular links are

$$\mathbb{P}_{\mathcal{W}}^x(T) = \frac{\pi\delta\lambda_x \left(\frac{\sigma^2}{P_x}\right)^{\delta/2} \nu T^\nu}{\Phi} \int_0^\infty \frac{H_{1,1}^{1,0} \left[\left(\frac{T}{\xi}\right)^\nu \frac{1}{\Phi} \middle| \begin{matrix} (1-\nu, \nu) \\ (0, 1) \end{matrix} \right]}{\xi^{\nu+1+\frac{\delta}{2}}} \times H_{1,1}^{1,1} \left[\pi\lambda_x (1 + \mathcal{G}_x) \frac{\left(\frac{\sigma^2}{P_x}\right)^\delta}{\xi^\delta} \middle| \begin{matrix} (1-\delta, \delta) \\ (0, 1) \end{matrix} \right] d\xi \quad (10)$$

where $x \in \{c, d\}$, and

$$\begin{cases} \mathcal{G}_d = \xi^\delta \Phi^{\frac{\delta}{\nu}} \Gamma(1-\delta) \Gamma\left(1 + \frac{\delta}{\nu}\right), \\ \mathcal{G}_c = \frac{\delta}{1-\delta} H_{3,3}^{3,1} \left[\frac{1}{\xi\Phi^{\frac{1}{\nu}}} \middle| \begin{matrix} (-1, 1), (1-\delta, 1), (1, 1) \\ (1, \frac{1}{\nu}), (-\delta, 1), (0, 1) \end{matrix} \right]. \end{cases} \quad (11)$$

Proof: See Appendix C for details.

Corollary 2 (Limits of Network Densification in Weibull Fading): For any SINR target T , the cellular coverage probability in Weibull fading flattens out starting from some network density λ_c as

$$\lim_{\lambda_c \rightarrow \infty} \mathbb{P}_{\mathcal{W}}^c(T) = \frac{\nu T^\nu \left(\frac{P_c}{\sigma^2}\right)^{\delta/2}}{\Phi} \int_0^\infty \frac{\xi^{\frac{\delta}{2}-\nu-1} H_{1,1}^{1,0} \left[\left(\frac{T}{\xi}\right)^\nu \frac{1}{\Phi} \middle| \begin{matrix} (1-\nu, \nu) \\ (0, 1) \end{matrix} \right]}{1 + \frac{\delta}{1-\delta} H_{3,3}^{3,1} \left[\frac{1}{\xi\Phi^{\frac{1}{\nu}}} \middle| \begin{matrix} (-1, 1), (1-\delta, 1), (1, 1) \\ (1, \frac{1}{\nu}), (-\delta, 1), (0, 1) \end{matrix} \right]} d\xi. \quad (12)$$

Proof: The result follows in the same line of (7) while using (10).

The D2D SIR distribution is obtained from (48) as

$$\mathbb{P}_{\mathcal{W}}^{d,\sigma \approx 0}(T) \stackrel{(a)}{=} \mathcal{E}_r \left[\text{H}_{1,2}^{2,0} \left[\pi \lambda_d \kappa_{\mathcal{W}} T^\delta r^2 \left| \begin{matrix} (1, \delta) \\ (0, 1), (1, \frac{\delta}{\nu}) \end{matrix} \right. \right] \right] \quad (13)$$

where (a) follows from applying [19, Eqs. 2.3] whereby $\kappa_{\mathcal{W}} = \Gamma(1 - \delta)\Gamma(1 + \frac{\delta}{\nu})$.

Remark 1: The Rayleigh fading is a special case of (46) and (48) when $m = 1$ and $\nu = 1$, respectively, thereby yielding

$$\mathbb{P}^x(T) \stackrel{(a)}{=} \pi \delta \lambda_x \left(\frac{\sigma^2}{P_x} \right)^{\delta/2} \text{H}_{1,1}^{1,1} \left[\pi \lambda_x (1 + \mathcal{R}_x) \frac{\left(\frac{\sigma^2 \Omega}{P_x} \right)^\delta}{T^\delta} \left| \begin{matrix} (1 - \delta, \delta) \\ (0, 1) \end{matrix} \right. \right] \quad (14)$$

with

$$\left\{ \begin{array}{l} \mathcal{R}_d = \frac{\pi T^\delta}{\delta \sin(\pi \delta)}, \\ \mathcal{R}_d = \frac{T^\delta}{1 - \delta} {}_2F_1(1 - \delta, 1; 2 - \delta; -T), \end{array} \right. \quad (15)$$

where (a) follows after recognizing that $\text{H}_{1,1}^{1,0} \left[x \left| \begin{matrix} 1 \\ 1 \end{matrix} \right. \right] = \delta[x - 1]$, when $\delta[x]$ stands for the DiracDelta function, i.e., $\delta[x] = 0; x \neq 0$. The coverage formulas in (14) matches the well-known major results for Rayleigh fading obtained in [6, Theorem 1] with the valuable add-on of being in closed-form.

IV. AREA SPECTRAL EFFICIENCY OPTIMIZATION

Hereafter, we consider a cellular network underlaid with D2D TxS. We assume an ALOHA-type channel access for both D2D and cellular TxS with probability p_d and p_c , respectively. Then, the set of active MBS/D2D TxS also forms a HPPP $\Psi_i^{\{TX\}}$ with density $\lambda_i p_i$ where $i \in \{c, d\}$. We assume that each cellular transmitter has its intended receiver at a fixed distance r_c in a random direction. Similarly, each D2D receiver is located at distance r_d from its corresponding transmitter.

The ASE, often referred to as network throughput, is a measure of the number of users that can be simultaneously supported by a limited radio frequency bandwidth per unit area.

Definition 2: In D2D-underlaid cellular networks, the ASE of D2D communications can be expressed as [17]

$$\mathcal{T}(T_d) = p_d \lambda_d \mathbb{P}(\text{SINR}_d(P_d) > T_d) \log_2(1 + T_d), \quad (16)$$

where $\mathbb{P}(\text{SINR}_d > T_d) = \mathbb{P}^d(T_d)$ is the mean of the D2D coverage probability (previously derived in Section III), $p_d \lambda_d$ denotes the effective D2D link density without any inactive D2D link, and p_d is the access probability.

In what follows, capitalizing on the statistical framework developed in section III, we present quality-based power control strategies for D2D communications under both Nakagami- m and Weibull fading channels aiming to reduce the interference caused by D2D TxS and to maximize the ASE of D2D communications.

A. Cellular Coverage Probability-Aware Power Control

Consider an arbitrary cellular transmitter $x \in \Psi_c^{\{TX\}}$ and its associated receiver at distance r_c . We are interested in investigating the joint effect of the interference coming from the surrounding BS and the D2D TxS on the downlink coverage probability while ignoring the noise by assuming $\sigma^2 = 0$. Therefore the SIR at the cellular receiver is expressed as

$$\text{SIR}_c(P_d) = \frac{h_c r_c^{-\frac{2}{\alpha}}}{\sum_{i \in \Psi_c^{\{TX\}} \setminus \{0\}} h_i r_i^{-\frac{2}{\alpha}} + \eta \sum_{j \in \Psi_d^{\{TX\}}} h_j r_j^{-\frac{2}{\alpha}}} = \frac{h_c r_c^{-\frac{2}{\alpha}}}{I_c + \eta I_d}, \quad (17)$$

where $\eta = \frac{P_d}{P_c}$ is the ratio of the transmit powers of the D2D. Let ρ_{th}^c be the operator-specified cellular success probability threshold. The maximum transmit power for D2D TxS is obtained by solving the following optimization problem:

$$\begin{array}{ll} \max & P_d \\ \text{s.t.} & \mathbb{P}(\text{SIR}_c(P_d) > T_c) \geq \rho_{th}^c, \end{array} \quad (18)$$

where for any P_d , the cellular coverage probability, conditioned on r_c , can be expressed over general fading based on (17) and employing (2) as

$$\mathbb{P}(\text{SIR}_c(P_d) > T_c) = \mathbb{P}^c(T_c)|_{r_c} = \frac{1}{T_c} \int_0^\infty \Phi(\xi, T_c) \exp(-\mathcal{A}^c(\xi r_c^2, \delta) - \eta^\delta \mathcal{A}^d(\xi r_c^2, \delta)) d\xi, \quad (19)$$

where $\Phi(\xi, T_c)$ is a function of only the fading parameters as previously shown in (46) and (48). Moreover, assuming that the distance-based association policy imposes no constraint on the location of interfering MBSs to the probe receiver, we have

$$\mathcal{A}^x(\xi, \delta) = \pi p_x \lambda_x \mathcal{E}[h_x^\delta] \Gamma(1 - \delta) \xi^\delta, \quad x \in \{c, d\}, \quad (20)$$

1) *D2D Power Control Under Nakagami- m Fading:* In this section, we assume that all links experience Nakagami- m flat fading channel. The fading severity of the Nakagami- m channel is captured by the parameter m_d for all links originating from the D2D transmitters, while the fading severity of the cellular communication and interference links is captured by the parameter m_c .

Proposition 3: The maximum D2D transmit power can be expressed under Nakagami- m fading as

$$\eta p_d^{\frac{1}{\delta}} = \max \left\{ \left(\frac{-p_c \lambda_c \kappa_m^c}{\lambda_d \kappa_m^d \left(\frac{m_c}{m_d} \right)^\delta} + \frac{(1 - m_c) \mathcal{W} \left(\frac{(\rho_{th}^c \Gamma(m_c))^{\frac{1}{m_c - 1}}}{m_c - 1} \right)}{\pi T_c^\delta r_c^2 \lambda_d \kappa_m^d \left(\frac{m_c}{m_d} \right)^\delta} \right)^{\frac{1}{\delta}}, 0 \right\}, \quad (21)$$

which acts as an average individual interference budget of each D2D Tx to guarantee the coverage probability of cellular users, where $\kappa_m^x = \frac{\Gamma(1 - \delta)\Gamma(m_x + \delta)}{\Gamma(m_x)}$, $x \in \{d, c\}$ and $\mathcal{W}(\cdot)$ is the principal branch of the Lambert function [21].

Proof: The cellular coverage probability under Nakagami- m fading follows from (19) as

$$\begin{aligned} \mathbb{P}_m^c(T_c)|_{r_c} &\stackrel{(a)}{=} \frac{1}{\Gamma(m_c)} \\ &\times H_{1,2}^{2,0} \left[T_c^\delta r_c^2 \left(p_d \lambda_d \kappa_m^d \left(\frac{m_c}{m_d} \right)^\delta \eta^{\delta + p_c \lambda_c \kappa_m^c} \right) \middle| (0, 1), (m_c, \delta) \right] \\ &\stackrel{(b)}{\approx} \frac{T_c^{\delta(m_c-1)} \left(p_d \lambda_d \kappa_m^d \left(\frac{m_c}{m_d} \right)^\delta \eta^{\delta + p_c \lambda_c \kappa_m^c} \right)^{m_c-1}}{\Gamma(m_c)} \\ &\underset{T_c \rightarrow \infty}{\approx} e^{-T_c^\delta r_c^2 \left(p_d \lambda_d \kappa_m^d \left(\frac{m_c}{m_d} \right)^\delta \eta^{\delta + p_c \lambda_c \kappa_m^c} \right)}, \end{aligned} \quad (22)$$

where (a) follows from (8) while \mathcal{A}_m^d is given in (47) and $\mathcal{A}_m^c = \mathcal{A}_m^d(m_d \leftarrow m_c, p_d \leftarrow p_c)$.

Definition 3: Consider the Fox's-H function defined by [25, Eq. (1.1.1)]. Its asymptotic expansion near $x = \infty$ when $n = 0$ is given by [25, Eq. (1.7.14)]

$$H_{p,q}^{q,0}(x) \sim x^{\frac{\nu+\frac{1}{2}}{\Delta}} \exp \left[-\Delta \left(\frac{x}{\rho} \right)^{1/\Delta} \right], \quad (23)$$

where ν , Δ , and ρ are constants defined in [25, Eq. (1.1.8)], [25, Eq. (1.1.9)], and [25, Eq. (1.1.10)], respectively. Then (b) follows after recognizing that $\delta = 1$, $\rho = 1$, $\nu = m_c - \frac{3}{2}$. Finally, solving (22)(b)- $\rho_{th}^c = 0$ yields the desired result after some mathematical manipulations.

2) *D2D Power Control Under Weibull Fading:* In this section, we assume that all links experience Weibull flat fading channel. Specifically, the cellular interfering link suffers from the Weibull (ν_c) fading and the D2D interference link experiences the Weibull (ν_d) fading.

Proposition 4: The cellular success probability-aware power control under Weibull fading yields

$$\eta p_d^{\frac{1}{\delta}} = \max \left\{ \left(-\frac{p_c \lambda_c \kappa_{\mathcal{W}}^c}{\lambda_d \kappa_{\mathcal{W}}^d} + \frac{\rho_c \left(-\frac{\ln(\rho_{th}^c)}{\sigma_c} \right)^{1/\sigma_c}}{\pi \lambda_d \kappa_{\mathcal{W}}^d T_c^\delta r_c^2} \right)^{\frac{1}{\delta}}, 0 \right\}, \quad (24)$$

where $\kappa_{\mathcal{W}}^x = \Gamma(1-\delta)\Gamma(1+\frac{\delta}{\nu_x})$, $x \in \{d, c\}$, $\sigma_c = 1+\delta(1-\frac{1}{\nu_c})$, and $\rho_c = \delta^{-\delta} \left(\frac{\delta}{\nu_c} \right)^{\delta/\nu_c}$.

Proof: The cellular coverage probability under Weibull fading follows from (19) as

$$\begin{aligned} \mathbb{P}_{\mathcal{W}}^c(T_c)|_{r_c} &\stackrel{(a)}{=} \\ &H_{1,2}^{2,0} \left[T_c^\delta r_c^2 \left(p_d \lambda_d \kappa_{\mathcal{W}}^d \eta^\delta + p_c \lambda_c \kappa_{\mathcal{W}}^c \right) \middle| (0, 1), (1, \frac{\delta}{\alpha_c}) \right], \\ &\stackrel{(b)}{\approx} \underset{T_c \rightarrow \infty}{\approx} e^{-\sigma_c \left(\frac{T_c^\delta r_c^2 \left(p_d \lambda_d \kappa_{\mathcal{W}}^d \eta^{\frac{\delta}{\alpha_c}} + p_c \lambda_c \kappa_{\mathcal{W}}^c \right)}{\rho_c} \right)^{1/\sigma_c}}, \end{aligned} \quad (25)$$

where (a) follows from applying (48) whereby $\mathcal{A}_{\mathcal{W}}^d$ is given in (49) and $\mathcal{A}_{\mathcal{W}}^c = \mathcal{A}_{\mathcal{W}}^d(\nu_d \leftarrow \nu_c, p_d \leftarrow p_c)$. Moreover (b) follows from resorting to (23). Subsequently, by solving (25)(b)- $\rho_{th}^c = 0$, we get (24) after some mathematical manipulations.

In reality, the individual interference budgets in (21) and (24) may be calculated and broadcast by MBSs to each D2D

Tx at the initial stage. In order to use the licensed spectrum, each D2D Tx must obey the individual interference budget in its power allocation stage. Note that our problem formulation is based on the distributed power control framework where cellular users and D2D Txs do not need to share location or channel state, which implies that the individual interference budget in (21) and (24) do not require the instantaneous CSI which is in fact difficult to get accurately especially upon high mobility of cellular and D2D users. Under the proposed distributed power allocation framework, a D2D Tx selects its transmit power based solely on the knowledge of the cross-tier communication distance r_c , the users and MBS spatial density, and the joint effect of path loss and fading. Compared to most existing schemes for D2D power control that are based on the real-time CSI to mitigate interference ([16] and references therein), the proposed power control framework, being statistically featured, does not burden the network latency.

In particular, from (21) and (24) we prove that the cellular user coverage probability guarantee can be distributively satisfied regardless of whether the D2D transmitters adapt their transmit power or access probability. In other words, D2D users can tune either of these two parameters representing an interference budget that each D2D pair may not exceed toward the cellular users.

B. D2D ASE-Aware Access Probability

In densely deployed D2D networks, both D2D to cellular and inter-D2D interferences would be very high. As a result, the cellular coverage probability threshold may not be guaranteed, even under individual D2D interference budget, especially when the target cellular SIR threshold is high. Hereafter, instead of allowing all D2D transmitters to access the channels, a part of D2D pairs cannot access the network to decrease interferences. Hence we propose to extend the cellular coverage probability-aware power control by integrating it with opportunistic access control to maximize the area spectral efficiency of D2D communications while decreasing both inter-D2D and cross-tier interferences.

After obeying to the individual interference budget in its power allocation stage, each D2D Tx maximizes its ASE utility $\mathcal{T}(T_d)$ by optimizing the access probability p_d . We formulate the individual access-aware design problem of D2D Tx as

$$\begin{aligned} &\max_{p_d} \mathcal{T}(T_d) \\ &\text{s.t. } 0 < p_d \leq 1, \end{aligned} \quad (26)$$

where $\mathcal{T}(T_d)$ is defined in (16) with maximum permissible transmit power for an arbitrary D2D user at a particular MAP p_d obtained from (21), and $\mathbb{P}^d(P_d, p_d)$ is the SIR coverage probability of an arbitrary D2D link obtained as

$$\begin{aligned} \mathbb{P}^d(T_d)|_{r_d} &\triangleq \mathbb{P} \left(\text{SIR}_d = \frac{h_d r_d^{-\frac{2}{\delta}}}{\eta^{-1} I_c + I_d} \geq T_d \right) \\ &= \frac{1}{T_d} \int_0^\infty \Phi(\xi, T_d) \exp(-\eta^{-\delta} \mathcal{A}^c(\xi r_d^2, \delta) - \mathcal{A}^d(\xi r_d^2, \delta)) d\xi, \end{aligned} \quad (27)$$

1) *D2D ASE under Nakagami- m Fading*: Under Nakagami- m fading, and conditioned on r_d , the SIR coverage probability of an arbitrary D2D link under transmit power adaptation (i.e., considering (21)) follows from applying (27) while considering (8) as

$$\begin{aligned} \mathbb{P}_m^d(T_d)|_{P_d^*} &= \frac{1}{\Gamma(m_d)} \\ &\times \mathbb{H}_{1,2}^{2,0} \left[p_d \lambda_d \kappa_m^d T_d^\delta r_d^2 \Xi \left| \begin{matrix} (1, \delta) \\ (0, 1), (m_d, \delta) \end{matrix} \right. \right] \\ &\stackrel{(a)}{\approx} \frac{(p_d \lambda_d \kappa_m^d T_d^\delta r_d^2 \Xi)^{m_d-1}}{\Gamma(m_d)} e^{-p_d \lambda_d \kappa_m^d T_d^\delta r_d^2 \Xi} \Big|_{\Xi_1}, \end{aligned} \quad (28)$$

where P_d^* is the maximum D2D transmit power of D2D Tx identified by cellular success probability-aware power control,

$$\Xi = \left(1 - \frac{p_c \lambda_c \kappa_m^c T_c^\delta r_c^2}{(1 - m_c) \mathcal{W} \left(-\frac{(\rho_{th}^c \Gamma(m_c))^{\frac{1}{m_c-1}}}{m_c-1} \right)} \right)^{-1}, \quad (29)$$

and (a) follows from applying the algebraic asymptotic expansions of the Fox's-H function in (23) with several mathematical manipulations.

Based on (32), (26) can be transformed further to

$$\begin{aligned} \max_{p_d} \quad & p_d^{m_d} e^{-p_d \Xi_1} \\ \text{s.t.} \quad & 0 < p_d \leq 1, \end{aligned} \quad (30)$$

where $\Xi_1 = \kappa_m^d T_d^\delta r_d^2 \Xi$.

Proposition 5: The optimal access probability p_d^* under Nakagami- m fading verifies

$$\frac{\partial p_d^{m_d} e^{-p_d \Xi_1}}{\partial p_d} = 0, \quad (31)$$

and is easily decided, after some manipulations, by

$$p_d^* = \min \left\{ \frac{m_d}{\lambda_d \kappa_m^d T_d^\delta r_d^2 \Xi}, 1 \right\}. \quad (32)$$

The D2D area spectral efficiency when operating at (P_d^*, p_d^*) can be quantified under Nakagami- m fading as

$$\mathcal{T}_d^*|_{p_d^*} \approx \frac{p_d^{m_d} e^{-m_d} \log_2(1 + T_d)}{\Gamma(m_d) \kappa_m^d T_d^\delta r_d^2 \Xi}, \quad (33)$$

where $e \simeq 0.277$.

2) *D2D ASE under Weibull Fading*: The area spectral efficiency of D2D underlay cellular networks under Weibull fading and cellular success probability-aware power control (i.e., considering (24)) can be expressed as

$$\mathcal{T}_d|_{p_d} \approx p_d \lambda_d \log_2(1 + T_d) \exp \left(-\sigma_d \left(p_d \frac{\lambda_d \kappa_{\mathcal{W}}^d T_d^\delta r_d^2 \Pi}{\rho_d} \right)^{1/\sigma_d} \right), \quad (34)$$

where $\sigma_d = 1 + \delta(1 - \frac{1}{\nu_d})$, $\rho_d = \delta^{-\delta} \left(\frac{\delta}{\nu_d} \right)^{\delta/\nu_d}$, and

$$\Pi = \left(1 - \frac{\lambda_c \kappa_{\mathcal{W}}^c T_c^\delta r_c^2}{\rho_c \left(-\frac{\ln(\rho_{th}^c)}{\sigma_c} \right)^{1/\sigma_c}} \right)^{-1}. \quad (35)$$

Proof: Following the same rationale to obtain (32), while considering (24), yield the success probability of D2D underlay network under Weibull fading with maximum permissible transmit power. Plugging the obtained result into (16) completes the proof.

Proposition 6: The optimal access probability (p_d^*) which maximizes the area spectral efficiency for D2D underlay network under cellular success probability-aware power control operating over Weibull fading verifies

$$1 - (\Pi_1 p_d)^{1/\sigma_d} = 0, \quad 0 < p_d \leq 1, \quad (36)$$

obtained from the maximization of the area spectral efficiency in (34), thereby yielding

$$p_d^* = \min \left\{ \frac{\rho_d \left(1 - \frac{\lambda_c \kappa_{\mathcal{W}}^c T_c^\delta r_c^2}{\rho_c \left(-\frac{\ln(\rho_{th}^c)}{\sigma_c} \right)^{1/\sigma_c}} \right)}{\lambda_d \kappa_{\mathcal{W}}^d T_d^\delta r_d^2}, 1 \right\}. \quad (37)$$

Plugging p_d^* into (34) yields the D2D underlay network ASE with cellular success probability-aware power control and opportunistic access control under Weibull fading as

$$\mathcal{T}_d^*|_{p_d^*} \approx \frac{\rho_d e^{-\sigma_d} \log_2(1 + T_d)}{\kappa_{\mathcal{W}}^d T_d^\delta \Pi} = \frac{\rho_d e^{-\sigma_d} \log_2(1 + T_d)}{\Gamma(1 - \delta) \Gamma(1 + \frac{\delta}{\nu_d}) T_d^\delta r_d^2 \Pi}. \quad (38)$$

Note that both the optimal access probability and ASE are inversely proportional to the D2D link distance r_d . That is implying that a D2D Tx with a short communication distance has a higher access probability than a D2D transmitter with a larger communication distance, because it has a potentially higher SIR. We also notice that p_d^* is inversely related to the density of D2D users (λ_d). Notice that in many studies that intrinsically rely on the optimality of access or power against density adaptation [26], a similar behavior was noticed. However, in this paper, we show that both the access and transmit power adaptations by themselves are sub-optimal. To overpass such suboptimality, we extend cellular success probability-aware power control by integrating it with opportunistic access control to maximize the area spectral efficiency of D2D communications.

Note that (33) and (38) coincide when $m_d = m_c = 1$ and $\nu_c = \nu_d = 1$ corresponding to the Raleigh case.

V. NUMERICAL AND SIMULATION RESULTS

In this section, numerical examples are shown to substantiate the accuracy of the new unified mathematical framework and to explore from our new analysis the effects of both the link- and network- level dynamics² on the ASE of the underlay D2D network.

Fig. 1 shows the ASE of the D2D underlay network under Nakagami- m fading as a function of the D2D transmit power. We can notice that D2D transmitters can increase their transmit power to improve D2D receivers' ASE up to a maximum value

²Link-level dynamics correspond to the uncertainty experienced due to multi-path propagation and topological randomness, while network-level dynamics are shaped by medium access control, device/BS density, etc.

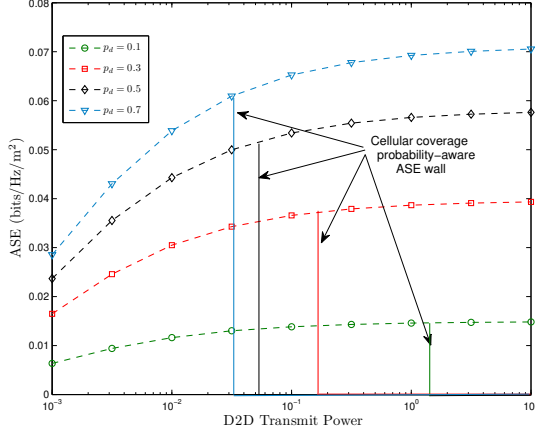


Fig. 1. ASE of a D2D underlay network with transmit power control under Nakagami- m fading with $\lambda_d = 10^{-2}$, $\lambda_c = 10^{-3}$, $P_c = 1$, $\alpha = 4$, $r_c = r_d = 1$, $\rho_{th}^c = 0.1$, $p_c = 0.4$, $m_c = m_d = 1.5$, $T_c = 5$ dB, and $T_d = 3$ dB.

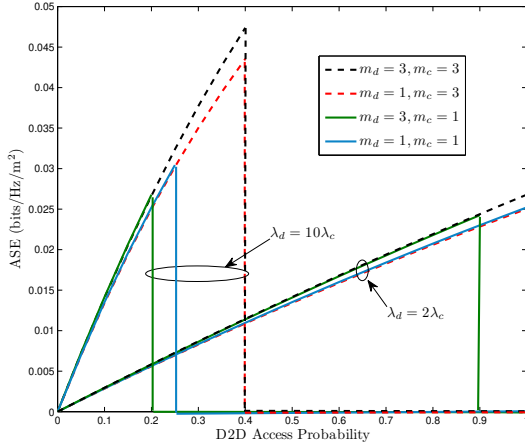


Fig. 2. ASE of a D2D underlay network with access control under Nakagami- m fading with $\lambda_c = 10^{-3}$, $P_c = 1$, $P_d = 0.1$, $\alpha = 4$, $r_c = r_d = 1$, $\rho_{th}^c = 0.1$, $p_c = 0.4$, $T_c = 5$ dB, and $T_d = 3$ dB.

beyond which the operation becomes unfeasible due to the bound enforced by the cellular network. Fig. 1 also shows that transmit power and access probability play a dual role. Indeed, an increase in the operational access probability inflicts a higher co-channel interference to the cellular user and, hence, a more stringent operational constraint by a reduction in the individual D2D interference budget (the maximum permissible transmit power) and thereby of the ASE. Hence the gain obtained due to an increase in the simultaneous transmissions may vanish because of the reduction in the success probabilities of the individual links. This indicates that there may exist an optimal operational point where the reduction in the link coverage can be balanced by increasing the number of concurrent transmissions.

Fig. 2 plots the ASE of the D2D underlay network under Nakagami- m fading as a function of the D2D mean access probability. We observe that the maximum permissible density

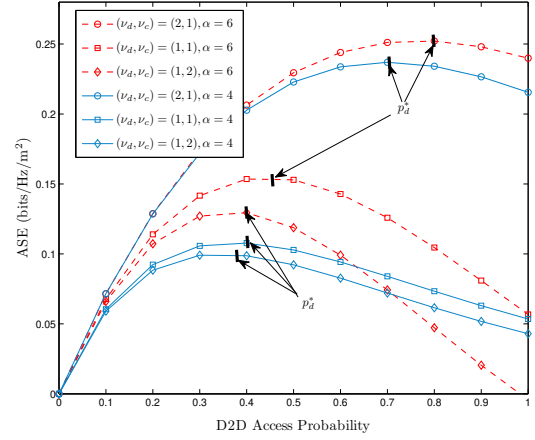


Fig. 3. Impact of the path-loss exponent on the ASE of the D2D underlay network under Weibull fading with $\lambda_d = 10^{-2}$, $\lambda_c = 10^{-3}$, $P_c = 1$, $r_c = r_d = 1$, $\rho_{th}^c = 0.1$, $p_c = 0.4$, $T_c = 5$ dB, and $T_d = 3$ dB.

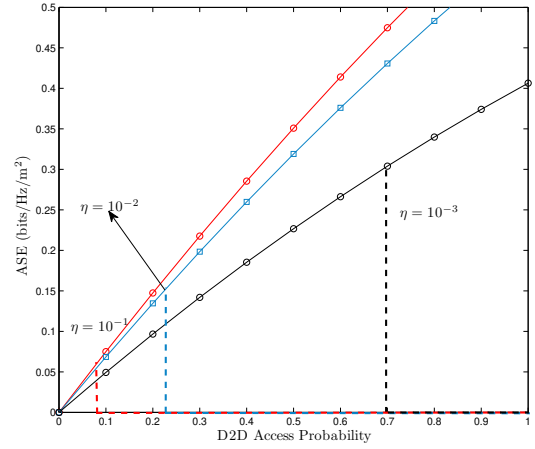


Fig. 4. ASE under Weibull fading for various value of η with $\lambda_d = 10^{-2}$, $\lambda_c = 10^{-3}$, $P_c = 1$, $\alpha = 4$, $r_c = r_d = 1$, $\rho_{th}^c = 0.1$, $p_c = 0.4$, $\nu_c = \nu_d = 2.5$, $T_c = 5$ dB, and $T_d = 3$ dB.

of the active D2D transmitters is bounded due to the cellular user's coverage constraint, thereby consolidating the trends of Fig. 1. Fig. 2 further investigates the impact of cellular and D2D channel fading severities and user densities on the ASE. For almost equally densely deployed cellular and D2D networks, D2D performance is governed by the fading severity m_c rather than m_d . In this case, cellular users employ higher transmit power thereby bounding the D2D underlay network performance due to the inflicted cellular interference. The dominant fading severity parameter is reversed when $\lambda_d > \lambda_c$ which is hardly surprising because the increased density limits the D2D network's performance by its own co-channel interference. In brief, Fig. 2 stipulates that the ASE of D2D networks is jointly dependent on the density of users and the propagation conditions.

Fig. 3 depicts the ASE of the D2D underlay network as a function of the D2D mean access probability under Weibull

fading. As observed in Fig. 3 the ASE is strongly coupled with the fading severity of the propagation channel. For a D2D network more densely deployed than the cellular network ($\lambda_d > \lambda_c$), the fading severity ν_d plays a more important role than ν_c . Hence, the attainable ASE is dramatically reduced when the fading severity of inter-tier D2D communication and cross-tier interference channel is reduced. In fact, a reduced power budget due to an increased fading parameter (small fading severity) outweighs the performance gain due to better propagation conditions for the communication link.

Fig. 4 plots the ASE in Weibull fading for several different values of η against the D2D mean access probability. We observe that reducing η enlarges the D2D operational region in terms of access probability at smaller ASE values. This is in fact due to less cross-tier interference with a reduced signal power at the D2D receiver. Consequently, although a smaller η may increase the access probability limit, the attained performance may deteriorate due to the reduction of the overall ASE.

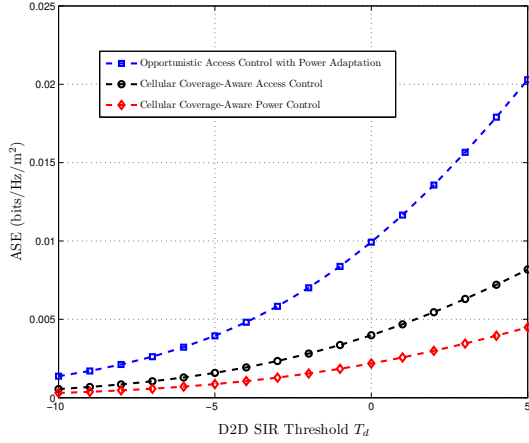


Fig. 5. ASE for D2D network according to different access and power control methods under Weibull fading with $\lambda_d = 10^{-2}$, $\lambda_c = 10^{-3}$, $P_c = 1$, $\alpha = 4$, $r_c = 5$, $r_d = 1$, $\rho_{th}^c = 0.7$, $\nu_c = \nu_d = 2.5$, $T_c = 10$ dB

Fig. 5, compares the performance of the cellular coverage-aware power or access control and the opportunistic access control combined with cellular coverage-aware power control. We notice that the latter scheme greatly improves the ASE of D2D communications comparing to sole adaptation of a single degree of freedom (transmit power or access probability) with an arbitrary selection of the other resulting in a sub-optimal performance. On the other hand, the maximum ASE under cellular coverage-aware access control is higher than the one attained with power control. However, the maximum ASE is bounded by a wall due to the primary user's QoS requirements.

VI. CONCLUSION

In this paper, we developed a new methodology for modeling and analyzing D2D-enabled cellular networks over general fading channels that relies on the H-transform theory. This methodology subsumes most known fading models and more importantly enables the unified analysis for the SINR distribution of D2D communications. This framework is traditionally

intractable due to the model-dependent limit on the distribution of the SINR in previous derivations. We build upon the developed statistical machinery to formulate an optimization scheme for D2D networks in terms of SIR and spectral efficiency. This scheme combines power control that is aware of cellular coverage probability with opportunistic access control. That is to reduce the interference caused by D2D communications and maximize the area spectral efficiency of D2D communications. We show that the optimal proportion and transmit power of active devices can be easily obtained by simple fading model-specific formulas, thereby serving as a useful tool for network designers to better understand and fine-tune the performance of D2D-enabled cellular networks.

VII. APPENDIX

A. Proof of Theorem 1:

The SINR CCDF $\mathbb{P}^x(T)$ may be retrieved from its Laplace transform as

$$\mathcal{L}^{\mathbb{P}^x}(z) = \frac{1}{z} - \frac{M_{\text{SINR}}^x(z)}{z}, \quad z \in \mathbb{R}_+, \quad (39)$$

where $M_{\text{SINR}}^x(z)$ denotes the SINR moment generating function recently derived in [9, Theorem 1]. Hence it follows that

$$\mathbb{P}^x(T) = 2 \int_0^\infty \mathcal{E}_h[\sqrt{h}\Upsilon] \mathcal{E}_r \left[\exp\left(-\frac{\sigma^2}{P} \xi^2 r^\alpha\right) \mathcal{L}_{\mathcal{I}_x}(\xi^2 r^\alpha) \right] d\xi, \quad (40)$$

where $\mathcal{L}_{\mathcal{I}_x}(s) = \mathcal{E}[e^{-s\mathcal{I}_x}]$ denotes the Laplace transform of the aggregate interference, and $\Upsilon = \mathcal{L}^{-1}\left(\frac{J_1(2\sqrt{sh}\xi)}{\sqrt{s}}, T\right)$, where $J_1(\cdot)$ is the Bessel function of the second kind [21, Eq. (8.402)] and $\mathcal{L}^{-1}(\cdot)$ stands for the inverse Laplace transform. Resorting to [19, Eq. (1.127)] and [19, Eq. (2.21)], we get

$$\Upsilon = \frac{\xi\sqrt{h}}{T} \mathbb{H}_{1,2}^{1,0} \left[\frac{h\xi^2}{T} \middle| \begin{matrix} (0,1) \\ (0,1), (-1,1) \end{matrix} \right]. \quad (41)$$

Plugging (41) into (40) and carrying out the change of variable relabeling ξ^2 as ξ yield

$$\begin{aligned} \mathbb{P}^x(T) &= \frac{1}{T} \int_0^\infty \mathcal{E}_h \left[h \mathbb{H}_{1,2}^{1,0} \left[\frac{h\xi}{T} \middle| \begin{matrix} (0,1) \\ (0,1), (-1,1) \end{matrix} \right] \right] \\ &\quad \mathcal{E}_r \left[\exp\left(-\frac{\sigma^2}{P} \xi^2 r^\alpha\right) \mathcal{L}_{\mathcal{I}}(\xi^2 r^\alpha) \right] d\xi. \end{aligned} \quad (42)$$

The Laplace transform of the interference at the cellular receiver, $\mathcal{L}_{\mathcal{I}_c}(s)$, is evaluated as follows

$$\mathcal{L}_{\mathcal{I}_c}(s) = \exp(2\pi\lambda_c\Theta(s)), \quad (43)$$

where

$$\begin{aligned} \Theta(s) &\stackrel{(a)}{=} \mathcal{E}_h \left[\int_r^\infty (1 - \exp(-sh_c x^{-\alpha})) x dx \right] \\ &\stackrel{(b)}{=} s\mathcal{E}_h \left[h \int_r^\infty x^{1-\alpha} e^{-sh_c x^{-\alpha}} {}_1F_1(1, 2, sh_c x^{-\alpha}) dx \right] \\ &\stackrel{(c)}{=} \frac{s\mathcal{E}_h \left[h {}_2F_2\left(1, \frac{2}{\alpha} + 1; 2; \frac{2}{\alpha} + 2; -sh_c r^{-\alpha}\right) \right]}{r^\alpha \alpha \left(1 - \frac{2}{\alpha}\right)}, \end{aligned} \quad (44)$$

and the PGFL of a HPPP with intensity function λ_c is used in the first equality, $(1 - e^{-x})/x = e^{-x} {}_1F_1(1, 2; x)$ is applied in (b), and (c) follows from letting $t = x^{-\alpha}$ and applying $\int x^{\beta-1} e^{-cx} {}_1F_1(a, b, cx) = \frac{x^\beta}{\beta} {}_2F_2(b-a, \beta, b, \beta+1, -cx)$.

The Laplace transform of the interference at the probe D2D receiver, $\mathcal{L}_{\mathcal{I}_d}(\xi)$, can be evaluated as [13, Eq. (22)]

$$\mathcal{L}_{\mathcal{I}_d}(\xi) = \exp(-\pi\lambda_d \xi^\delta \Gamma(1-\delta) \mathcal{E}[h^\delta]). \quad (45)$$

Finally, plugging (44) and (45) into (42) with simple algebraic manipulations, the final result presented in Theorem 1 follows.

B. Proof of Proposition 1:

Let h be a random variable with $f_h(y) = \frac{(\frac{m}{\Omega})^m}{\Gamma(m)} x^{m-1} e^{-\frac{m}{\Omega}x}$ put in the form of a single H-variate [19, Eq. (1.125)], then applying [21, Eqs. (7.813), (9.31.5)] yields $\Psi(\xi, T)$ after some manipulations. On the other hand, $\mathcal{A}_m^d(\xi, \alpha)$ is obtained from (3) while $\mathcal{E}[h^\delta] = \frac{\Gamma(m+\delta)}{\Gamma(m)} (\frac{\Omega}{m})^\delta$ and $\mathcal{A}_m^c(\xi, \alpha)$ follows from (3) after applying [21, Eq. (7.522.9)]. Plugging all these results in (2) and (3) yields

$$\begin{aligned} \mathbb{P}_m^x(T) &= \frac{1}{\Gamma(m)} \int_0^\infty \xi^{-1} \mathbb{H}_{2,2}^{1,1} \left[\frac{\Omega\xi}{mT} \middle| \begin{matrix} (1-m, 1) \\ (0, 1) \end{matrix} \right] \\ &\quad \times \mathcal{E}_r \left[\exp \left(-\frac{\sigma^2}{P_x} \xi r^\alpha - \mathcal{A}_m^x(\xi r^\alpha, \delta) \right) \right] d\xi, \end{aligned} \quad (46)$$

where

$$\begin{cases} \mathcal{A}_m^d(\xi, \delta) = \pi\lambda_d \xi^\delta \left(\frac{\Omega}{m}\right)^\delta \frac{\Gamma(1-\delta)\Gamma(m+\delta)}{\Gamma(m)}, \\ \mathcal{A}_m^c(\xi, \delta) = \frac{\pi\delta\lambda_c \xi \Omega}{r^{2(1/\delta-1)}(1-\delta)} {}_3F_2 \left(1-\delta, 1, m+1; 2-\delta, 2; -\frac{\Omega\xi}{mr^{2/\delta}} \right). \end{cases} \quad (47)$$

We assume that the distance r between a typical user and its associated MBS (cellular link) or D2D helper (D2D link) follows a Rayleigh distribution, i.e. $f_{r_x}(r) = 2\pi\lambda_x r e^{-\pi\lambda_x r^2}$, $r \geq 0$, $x \in \{c, d\}$ [6]. Hence, substituting $f_r(\cdot)$ for cellular and D2D users in (46) and resorting to [19, Eq. (2.3)] yield (4) after some manipulations.

C. Proof of Proposition 2:

The proof follows from (2) with $f_h(y) = \frac{\alpha}{\Phi} y^{\alpha-1} e^{-\frac{y^\alpha}{\Phi}} = \frac{\alpha}{\Phi} y^{\alpha-1} \mathbb{H}_{0,1}^{1,0} \left[\frac{y^\alpha}{\Phi} \middle| \begin{matrix} - \\ (0, 1) \end{matrix} \right]$ and applying [19, Eqs. (2.3), (1.56)]. Besides, $\mathcal{A}_{\mathcal{W}}^c(\xi, \alpha)$ follows by resorting to $\mathcal{E}[h^\delta] = \Gamma(1 + \frac{\delta}{\alpha}) \phi^{\frac{\delta}{\alpha}}$. On the other hand, recalling that ${}_pF_q(a_p; b_q; -z) = \mathbb{H}_{p,q+1}^{1,p} \left[z \middle| \begin{matrix} (1-a_p, 1) \\ (1, 1), (1-b_q, 1) \end{matrix} \right]$ and applying [19, Eqs. (2.3)] yield $\mathcal{A}_{\mathcal{W}}^c(\xi, \alpha)$ after some manipulations using the Fox-H function properties in [20, Eqs. (1.2.3), (1.2.4)]. Plugging all these results in (2) and (3) yields

$$\begin{aligned} \mathbb{P}_{\mathcal{W}}^x(T) &= \frac{\nu}{T\Phi} \int_0^\infty \left(\frac{T}{\xi}\right)^{\nu+1} \mathbb{H}_{1,1}^{1,0} \left[\left(\frac{T}{\xi}\right)^\nu \frac{1}{\Phi} \middle| \begin{matrix} (1-\nu, \nu) \\ (0, 1) \end{matrix} \right] \\ &\quad \times \mathcal{E}_r \left[\exp \left(-\frac{\sigma^2}{P_x} \xi r^\alpha - \mathcal{A}_{\mathcal{W}}^x(\xi r^\alpha, \delta) \right) \right] d\xi, \end{aligned} \quad (48)$$

where

$$\begin{cases} \mathcal{A}_{\mathcal{W}}^d(\xi, \delta) = \pi\lambda_d \xi^\delta \Phi^{\frac{\delta}{\alpha}} \Gamma(1-\delta) \Gamma(1 + \frac{\delta}{\alpha}), \\ \mathcal{A}_{\mathcal{W}}^c(\xi, \delta) = \frac{\delta\lambda_c r^2}{1-\delta} \mathbb{H}_{3,3}^{3,1} \left[\frac{r^{\frac{2}{\alpha}}}{\xi\Phi^{\frac{1}{\alpha}}} \middle| \begin{matrix} (-1, 1), (1-\delta, 1), (1, 1) \\ (1, \frac{1}{\nu}), (-\delta, 1), (0, 1) \end{matrix} \right]. \end{cases} \quad (49)$$

Finally, substituting $f_r(\cdot)$ for cellular and D2D users and proceeding as before completes the proof.

D. κ - μ and Shadowed κ - μ As Special Cases of the Degree-2 Fox's H-Function Fading Model

The κ - μ distribution, first introduced in [10], can be regarded as a generalization of the classic Rician fading model for LOS scenarios. Let h be a random variable statistically following a κ - μ distribution [27] with mean $\Omega = \mathcal{E}[h]$ and non-negative real shape parameters κ , and μ , with

$$f_h(x) = \frac{\mu \left(\frac{1+\kappa}{\Omega}\right)^{\frac{\mu+1}{2}} x^{\frac{\mu-1}{2}} e^{-\frac{\mu(1+\kappa)x}{\Omega}}}{e^{\kappa\mu} \kappa^{\frac{\mu-1}{2}}} \mathbb{I}_{\mu-1} \left(2\mu \sqrt{\frac{\kappa(1+\kappa)}{\Omega}} x \right), \quad (50)$$

where $\mathbb{I}_b(\cdot)$ stands for the modified Bessel function of the first kind of order b [21, Eq. (8.431.1)]. Recognizing that [19, A.7]

$$\mathbb{I}_\nu(z) = i^{-\nu} \mathbb{H}_{0,2}^{1,0} \left[-\frac{z^2}{4} \middle| \begin{matrix} \left(\frac{\nu}{2}, 1\right) \\ \left(-\frac{\nu}{2}, 1\right) \end{matrix} \right], \quad (51)$$

where $i^2 = -1$, then from (2) it follows that in κ - μ fading

$$\begin{aligned} \Psi(\xi, T) &= \mathcal{C}_{\kappa\mu} \int_0^\infty x^{\frac{\mu+1}{2}} e^{-\frac{\mu(1+\kappa)x}{\Omega}} \\ &\quad \times \mathbb{H}_{1,2}^{1,0} \left[\frac{\xi x}{T} \middle| \begin{matrix} (0, 1) \\ (0, 1), (-1, 1) \end{matrix} \right] \\ &\quad \times \mathbb{H}_{0,2}^{1,0} \left[-\frac{\mu^2 \kappa(1+\kappa)}{\Omega} x \middle| \begin{matrix} \left(\frac{\nu}{2}, 1\right) \\ \left(-\frac{\nu}{2}, 1\right) \end{matrix} \right] dx. \end{aligned} \quad (52)$$

The last H-transform is known as the Laplace transform of two Fox's-H function given by [20, Eq. (2.6.2)] as

$$\begin{aligned} \Psi(\xi, T) &= \mathcal{C}_{\kappa\mu} \left(\frac{\mu(1+\kappa)}{\Omega} \right)^{-\frac{\mu+3}{2}} \\ &\quad \mathbb{H}_{1,[0,1],0,[2,2]}^{1,0,0,1,1} \left[\begin{matrix} -\mu\kappa \\ \frac{\xi\Omega}{T\mu(1+\kappa)} \end{matrix} \middle| \begin{matrix} \left(1 + \frac{\mu+1}{2}, 1\right) \\ -; (0, 1) \\ \left(\frac{\mu-1}{2}, 1\right), \left(\frac{1-\mu}{2}, 1\right); (0, 1), (-1, 1) \end{matrix} \right], \end{aligned} \quad (53)$$

where $\mathbb{H}[\cdot, \cdot]$ denotes the generalized Fox's H-function of two variables [28, Eq. (1.1)] and it reduces with the help of [20, Eq. (2.3.1)] to the generalized Meijer's G-function of two variables. Recalling that $\mathcal{E}[h^j] = \frac{(\frac{\Omega}{\mu(1+\kappa)})^j \Gamma(\mu+j)}{e^{\mu\kappa}} {}_1F_1(\mu+j, \mu; -\mu\kappa)$ under κ - μ fading [13, Eq. (10)], thereby yielding $\mathcal{A}_{\kappa\mu}^d(\xi, \alpha)$ as in (56). On the other hand $\mathcal{A}_{\kappa\mu}^c(\xi, \alpha)$ is obtained from (3) using ${}_2F_2(1-\delta, 1; 2-\delta, 2; -\xi h) = \sum_{k=1}^2 {}_1F_1(a_k, a_k+1; -\xi h) \prod_{j=1, j \neq k}^3 \frac{a_j}{a_j - a_k}$ where $a_k \in \{1, 1-\delta\}$, $k = 1, \dots, 2$ then applying [29, Eq. (27)] yield

$$\begin{aligned} \Psi_1(a, b, c, c', w, z) &= \frac{\Gamma(c')}{\Gamma(a)} z^{\frac{1-c'}{2}} \int_0^\infty t^{a-\frac{1+c'}{2}} e^{-t} \mathbb{I}_{c'-1}(2\sqrt{tz}) \\ &\quad {}_1F_1(b, c, wt) dt, \end{aligned} \quad (54)$$

where $\Psi_1(\cdot, \cdot; \cdot, \cdot; \cdot, \cdot)$ stands for the Humbert function of the first kind [29, Eq. (2)]. Plugging all these result into (2) yields the D2D and cellular CCDFs as

$$\mathbb{P}_{\kappa\mu}^x(T) = \frac{\tilde{\mathcal{C}}_{\kappa\mu}}{T} \int_0^\infty G_{1,[0,1],0,[2,2]}^{1,0,0,1,1} \left[\begin{matrix} -\mu\kappa \\ \frac{\xi\Omega}{T\mu(1+\kappa)} \end{matrix} \middle| \begin{matrix} 1 + \frac{\mu+1}{2} \\ -; 0 \\ \frac{\mu-1}{2}, \frac{1-\mu}{2}; 0, -1 \end{matrix} \right] \times \mathcal{E}_r \left[\exp \left(-\frac{\sigma^2}{P_x} \xi r^\alpha - \mathcal{A}_{\kappa\mu}^x(\xi r^\alpha, \delta) \right) \right] d\xi, \quad (55)$$

where $\tilde{\mathcal{C}}_{\kappa\mu} = \frac{\mu(1+\kappa)^{\frac{\mu+1}{2}}}{e^{\kappa\mu}\Omega\kappa^{\frac{\mu-1}{2}}}$, and $\mathcal{A}_{\kappa\mu}^x(\xi, \alpha)$ is obtained as

$$\begin{cases} \mathcal{A}_{\kappa\mu}^d(\xi, \delta) = \frac{\pi\lambda_d\xi^\delta\Gamma(1-\delta)\left(\frac{\Omega}{\mu(1+\kappa)}\right)^\delta\Gamma(\mu+\delta)_1F_1(\mu+\delta, \mu; -\mu\kappa)}{\Gamma(\mu)}, \\ \mathcal{A}_{\kappa\mu}^c(\xi, \delta) = \frac{\delta\lambda_c\Omega\xi e^{-\mu\kappa} \sum_{k=1}^2 \Theta_k \Psi_1\left(\mu+1, a_k; a_k+1, \mu; \mu\kappa, -\frac{\xi\Omega}{\mu(1+\kappa)}\right)}{r^{2(1/\delta-1)}(1-\delta)}, \end{cases} \quad (56)$$

where $\Theta_k = \prod_{j=1, j \neq k}^2 \frac{a_j}{a_j - a_k}$ with $a_k \in \{1, 1-\delta\}$, $k = 1, \dots, 2$, and $G_{a,[c,e],b,[d,f]}^{p,q,k,r,l}[\cdot, \cdot]$ is the generalized Meijer's G-function of two variables [22].

In interference-limited κ - μ environment, the SIR CCDF of D2D links is obtained as

$$\begin{aligned} \mathbb{P}_{\kappa\mu}^d(T) &\stackrel{(a)}{=} \frac{\tilde{\mathcal{C}}_{\kappa\mu}}{T} \int_0^\infty G_{1,[0,1],0,[2,2]}^{1,0,0,1,1} \left[\begin{matrix} -\mu\kappa \\ \frac{\xi\Omega}{T\mu(1+\kappa)} \end{matrix} \middle| \begin{matrix} 1 + \frac{\mu+1}{2} \\ -; 0 \\ \frac{\mu-1}{2}, \frac{1-\mu}{2}; 0, -1 \end{matrix} \right] \\ &\times \mathcal{E}_r \left[H_{0,1}^{1,0} \left[\mathcal{A}_{\kappa\mu}^d(\xi r^\alpha, \delta) \middle| \begin{matrix} - \\ (0, 1) \end{matrix} \right] \right] d\xi \\ &= \delta\tilde{\mathcal{C}}_{\kappa\mu} \frac{(\lambda_d\kappa_{S\kappa\mu})^{-\frac{1}{\delta}}}{T} \mathcal{E}_r \left[r^2 \right. \\ &\left. H_{0,[2,2],1,[0,1]}^{1,1,2,0,0} \left[\begin{matrix} (-\mu\kappa)^{-\delta} \\ \lambda_d\kappa_{S\kappa\mu} T^\delta r^2 \end{matrix} \middle| \begin{matrix} (-\frac{\mu+1}{2}, \delta) \\ -; (\frac{1}{\delta}, 1); (1, \delta) \\ (\frac{3-\mu}{2}, \delta), (\frac{1+\mu}{2}, \delta); (1, \delta), (2, \delta) \end{matrix} \right] \right] \end{aligned} \quad (57)$$

where (a) follows from substituting $\mathcal{A}_{\kappa\mu}^d(\xi r^\alpha, \delta)$ by its expression in (56) after recognizing the Fox's-H representation of the exponential function [20, Eq. (1.7.2)] and employing [20, Eq. (2.11)]. Moreover, $\kappa_{S\kappa\mu} = \frac{\Gamma(1-\delta)\Gamma(\mu+\delta)e^{-\mu\kappa} {}_1F_1(\mu+\delta, \mu; -\mu\kappa)}{\Gamma(\mu)}$. Notice that the κ - μ includes the Rayleigh ($\kappa \rightarrow 0, \mu = 1$), Nakagami- m ($\kappa \rightarrow 0, \mu = m$), and Rician ($\kappa = K, \mu = 1$) fading models as special cases, where K is the Rician factor.

In shadowed κ - μ distribution the dominant signal components are subject to Nakagami- m shadowing with pdf [24, Table I]

$$f_{h,S\kappa-\mu}(y) = \frac{\mu^\mu m^m (1+\kappa)^\mu}{\Gamma(\mu)\Omega^\mu (\mu\kappa+m)^m} \left(\frac{y}{\Omega}\right)^{\mu-1} e^{-\frac{\mu(1+\kappa)}{\Omega}y} {}_1F_1\left(m, \nu, \frac{\mu^2\kappa(1+\kappa)}{\Omega(\mu\kappa+m)}y\right), \quad (58)$$

where ${}_1F_1(\cdot)$ denotes the confluent hypergeometric function of [21, Eq. (13.1.2)]. Recalling that

$${}_1F_1(a, b; z) = \frac{\Gamma(b)}{\Gamma(a)} {}_1F_{1,1} \left[-z \middle| \begin{matrix} (1-a, 1) \\ (0, 1), (1-b, 1) \end{matrix} \right], \quad (59)$$

then the D2D and cellular SINR CCDFs follow along the same line of (55) as

$$\mathbb{P}_{S\kappa\mu}^x(T) = \frac{\tilde{\mathcal{C}}_{S\kappa\mu}}{T} \int_0^\infty G_{1,[1,1],0,[2,2]}^{1,1,0,1,1} \left[\begin{matrix} \frac{\mu\kappa}{(\mu\kappa+m)} \\ \frac{\xi\Omega}{T\mu(1+\kappa)} \end{matrix} \middle| \begin{matrix} 1 + \mu \\ 1 - m; 0 \\ 0, 1 - \mu; 0, -1 \end{matrix} \right] \times \mathcal{E}_r \left[\exp \left(-\frac{\sigma^2}{P_x} \xi r^\alpha - \mathcal{A}_{S\kappa\mu}^x(\xi r^\alpha, \delta) \right) \right] d\xi, \quad (60)$$

where $\tilde{\mathcal{C}}_{S\kappa\mu} = \frac{\frac{\Omega}{\mu}}{\Gamma(m)(1+\kappa)\left(\frac{\mu\kappa}{m}+1\right)^m}$. Moreover in (60), $\mathcal{A}_{S\kappa\mu}^x(\xi, \alpha)$ is obtained as

$$\begin{cases} \mathcal{A}_{S\kappa\mu}^d(\xi, \delta) \stackrel{(a)}{=} \frac{\pi\lambda_d\xi^\delta\Gamma(1-\delta)\Gamma(\mu+\delta)_2F_1\left(\mu-m, \mu+\delta, \mu; -\frac{\mu\kappa}{m}\right)}{\left(\frac{\Omega}{\mu(1+\kappa)}\right)^{-\delta}\left(\frac{\mu\kappa}{m}+1\right)^{m-\mu-\delta}\Gamma(\mu)}, \\ \mathcal{A}_{S\kappa\mu}^c(\xi, \delta) \stackrel{(b)}{=} \frac{\delta\lambda_c\Omega\xi \sum_{k=1}^2 \Theta_k {}_2F_2\left(\mu+1, a_k, m; a_k+1, \mu; \frac{\mu\kappa}{\mu\kappa+m}, -\frac{\Omega\xi r^\alpha}{\mu(1+\kappa)}\right)}{r^{2(1/\delta-1)}(1+\kappa)(1-\delta)\left(\frac{\mu\kappa}{m}+1\right)^m}, \end{cases} \quad (61)$$

where (a) follows after recognizing that $\mathcal{E}[h^j] = \left(\frac{\Omega}{\mu(1+\kappa)}\right)^j \Gamma(\mu+j) \left(\frac{\mu\kappa}{m}+1\right)^{m-\mu-j} \Gamma(\mu) {}_2F_1\left(\mu-m, \mu+j, \mu; -\frac{\mu\kappa}{m}\right)$ [13, Eq. (10)] thereby yielding $\mathcal{A}_{S\kappa\mu}^d(\xi, \alpha)$. On the other hand, $\mathcal{A}_{S\kappa\mu}^c(\xi, \alpha)$ is obtained from (3) along the same line of (56) while considering the following integral form

$$F_2\left(a, b, b', c, c'; \frac{w}{p}, \frac{z}{p}\right) = \frac{p^a}{\Gamma(a)} \int_0^\infty x^{a-1} e^{-px} {}_1F_1(b, c, wx) {}_1F_1(b', c', xz) dx, \quad (62)$$

where $F_2(a, b, b'; c, c'; x, y)$ stands for the Appell's hypergeometric function of the second kind [30, Eq. (27)].

We assume that the communication is interference limited and hence thermal noise is negligible. Then the coverage of D2D communication in κ - μ shadowed fading is obtained as

$$\begin{aligned} \mathbb{P}_{S\kappa\mu}^d(T) &= \frac{\tilde{\mathcal{C}}_{S\kappa\mu}}{T} \int_0^\infty G_{1,[1,1],0,[2,2]}^{1,1,0,1,1} \left[\begin{matrix} \frac{\mu\kappa}{(\mu\kappa+m)} \\ \frac{\xi\Omega}{T\mu(1+\kappa)} \end{matrix} \middle| \begin{matrix} 1 + \mu \\ 1 - m; 0 \\ 0, 1 - \mu; 0, -1 \end{matrix} \right] \\ &\times \mathcal{E}_r \left[H_{0,1}^{1,0} \left[\mathcal{A}_{S\kappa\mu}^d(\xi r^\alpha, \delta) \middle| \begin{matrix} - \\ (0, 1) \end{matrix} \right] \right] d\xi \\ &= \delta\tilde{\mathcal{C}}_{S\kappa\mu} \frac{(\lambda_d\kappa_{S\kappa\mu})^{-\frac{1}{\delta}}}{T} \mathcal{E}_r \left[r^2 \right. \\ &\left. H_{0,[2,2],1,[1,1]}^{1,1,2,1,0} \left[\begin{matrix} \left(-\frac{\mu\kappa+m}{\mu\kappa}\right)^\delta \\ \lambda_d\kappa_{S\kappa\mu} T^\delta r^2 \end{matrix} \middle| \begin{matrix} (-\mu, \delta) \\ (m, \delta); (\frac{1}{\delta}, 1); (1, \delta) \\ (1, \delta), (\mu, \delta); (1, \delta), (0, \delta) \end{matrix} \right] \right], \end{aligned} \quad (63)$$

where $\kappa_{S\kappa\mu} = \frac{\Gamma(1-\delta)\Gamma(\mu+\delta)_2F_1\left(\mu-m, \mu+\delta, \mu; -\frac{\mu\kappa}{m}\right)}{\left(\frac{\mu\kappa}{m}+1\right)^{m-\mu-\delta}\Gamma(\mu)}$.

REFERENCES

- [1] M. N. Tehrani, M. Uysal, and H. Yanikomeroglu, "Device-to-device communication in 5G cellular networks: Challenges, solutions, and future directions," *IEEE Commun. Mag.*, vol. 52, no. 5, pp. 86-92, May 2014.
- [2] B. Bangerter, S. Talwar, R. Arefi, and K. Stewart, "Networks and devices for the 5G era," *IEEE Commun. Mag.*, vol. 52, no. 2, pp. 9096, 2014.
- [3] K. Doppler, M. Rinne, C. Wijting, C. B. Ribeiro, and K. Hugl, "Device-to-device communication as an underlay to LTE-advanced networks," *IEEE Commun. Mag.*, vol. 47, no. 12, pp. 42-49, Dec. 2009.
- [4] S.-Y. Lien, K.-C. Chen, and Y. Lin, "Toward ubiquitous massive accesses in 3GPP machine-to-machine communications," *IEEE Commun. Mag.*, vol. 49, no. 4, pp. 66-74, Apr. 2011.

- [5] H. Ilhan, M. Uysal, and I. Altunbas, "Cooperative diversity for intervehicular communication: Performance analysis and optimization," *IEEE Trans. Veh. Technol.*, vol. 58, no. 7, pp. 3301-3310, Sep. 2009.
- [6] X. Lin, J. G. Andrews, and A. Ghosh, "Spectrum sharing for device-to-device communication in cellular networks," *IEEE Trans. Wirel. Commun.*, vol. 13, no. 12, pp. 1-31, Dec. 2014.
- [7] G. George, R. K. Mungara, and A. Lozano, "An analytical framework for device-to-device communication in cellular networks," *IEEE Trans. Wireless Commun.*, vol. 14, no. 11, pp. 6297-6310, Nov. 2015.
- [8] H. ElSawy, E. Hossain, and M. S. Alouini, "Analytical modeling of mode selection and power control for underlay D2D communication in cellular networks," *IEEE Trans. Commun.*, vol. 62, no. 11, pp. 4147-4161, Nov. 2014.
- [9] I. Trigui, S. Affes, and B. Liang, "Unified stochastic geometry modeling and analysis of cellular networks in LOS/NLOS and shadowed fading," *IEEE Trans. Commun.*, vol. PP, no. 99, pp. 1-16, July 2017.
- [10] M. D. Yacoub, "The κ - μ distribution and the η - μ distribution," *IEEE Antennas Propag. Mag.*, vol. 49, no. 1, pp. 68-81, Feb. 2007.
- [11] N. Beaulieu and X. Jiandong, "A novel fading model for channels with multiple dominant specular components," *IEEE Wireless Commun. Lett.*, vol. 4, no. 1, pp. 54-57, Feb. 2015.
- [12] M. Peng, Y. Li, T. Q. S. Quek, and C. Wang, "Device-to-device underlaid cellular networks under rician fading channels," *IEEE Trans. Wirel. Commun.*, vol. 13, no. 8, pp. 4247-4259, Aug. 2014.
- [13] Y. J. Chun, S. L. Cotton, H. S. Dhillon, F. J. Lopez-Martinez, J. F. Paris, and S. Ki Yoo "A Comprehensive analysis of 5G heterogeneous cellular systems operating over κ - μ shadowed fading channels", CoRR, vol. arXiv:1609.09389, 2016. [Online].
- [14] S. Parthasarathy and R. K. Ganti, "Coverage analysis in downlink poisson cellular network with κ - μ shadowed fading," *IEEE Wireless Commun. Lett.*, vol. 6, no. 1, Feb. 2017.
- [15] Y. J. Chun, S. L. Cotton, H. S. Dhillon, A. Ghayeb, and M. O. Hasna, "A stochastic geometric analysis of device-to-device communications operating over generalized fading channels," *IEEE Trans. Wireless Commun.*, vol. 16, no. 7, pp. 4151-4165, Jul. 2017
- [16] N. Lee, X. Lin, J. G. Andrews, and R. W. Heath, "Power control for D2D underlaid cellular networks: Modeling, algorithms, and analysis," *IEEE J. Sel. Areas Commun.*, vol. 33, no. 1, pp. 113, Jan. 2015.
- [17] Z. Chen and M. Kountouris, "Distributed SIR-aware opportunistic access control for D2D underlaid cellular networks," in Proc. *IEEE Globecom*, Austin, TX, USA, pp. 1540-1545, Dec. 2014.
- [18] J. Park, and J. H. Lee, "Semi-distributed spectrum access to enhance throughput for underlay device-to-device communications", *IEEE Trans. Commun.*, vol. 65, no. 10, Oct. 2017.
- [19] M. Mathai, R. K. Saxena, and H. J. Haubold, *The H-function: Theory and Applications*, Springer, New York, 2010.
- [20] A. M. Mathai and R. K. Saxena, *The H-Function With Applications in Statistics and Other Disciplines*. New Delhi, India: Wiley Eastern, 1978.
- [21] I. S. Gradshteyn and I. M. Ryzhik, *Table of Integrals, Series and Products*, 5th ed., Academic Publisher, 1994.
- [22] R. U. Verma, "On some integrals involving Meijer's G-fuction of two variables", *Proc. Nat. Inst. Sci. India*, vol. 39, Jan. 1966.
- [23] M. K. Simon and M.-S. Alouini, *Digital Communication over Fading Channels*. Wiley-Interscience, 2005, vol. 95.
- [24] J. F. Paris, "Statistical Characterization of κ - μ Shadowed Fading," *IEEE Trans. Veh. Technol.*, vol.63, no. 2, pp. 518-526, Feb. 2014.
- [25] A. Kilbas and M. Saigo, *H-Transforms: Theory and Applications*, CRC Press, 2004.
- [26] H. Kobayashi, Y. Onozato, and D. Huynh, "An approximate method for design and analysis of an ALOHA system," *IEEE Trans. Commun.*, vol. 25, no. 1, pp. 148-157, 1977.
- [27] L. Moreno-Pozas, F. J. Lopez-Martinez, J. F. Paris, and E. Martos-Naya, "The κ - μ shadowed fading model: Unifying the κ - μ and η - μ distributions," *IEEE Trans. Veh. Technol.*, vol. 65, no. 12, pp. 9630-9341, Dec. 2016.
- [28] P. Mittal and K. Gupta, "An integral involving generalized function of two variables", *Proc. Ind. Acad. Sci.*, vol. 75, no. 3, pp. 117123, 1972.
- [29] Yu. A. Brychkova and N. Saad, "On some formulas for the Appell function $F_2(a, b, b'; c, c; w; z)$ ", *Integral Transforms and Special Functions*, vol. 25, no. 2, pp. 111-123, 2014.
- [30] S. B. Opps, N. Saad, and H.M. Srivastava, "Some reduction and transformation formulas for the Appell hypergeometric function F_2 " *Journal of Mathematical Analysis and Applications*, vol. 302, pp. 180-195, Feb. 2005.